Article

Not peer-reviewed version

Mitochondrial Function-Associated APOE Locus and its Implication in Alzheimer's Disease and Aging

Eun-Gyung Lee *, Lesley Leong, Sunny Chen, Jessica Tulloch, Chang-En Yu *

Posted Date: 28 April 2023

doi: 10.20944/preprints202304.1128.v1

Keywords: APOE locus; TOMM40; APOE; oxidative stress; mitochondrial dysfunction; mitochondrial DNA copy number; gene expression; Alzheimer's disease; aging

Article

Mitochondrial Function-Associated *APOE* Locus and Its Implication in Alzheimer's Disease and Aging

Eun-Gyung Lee [1,*], Lesley Leong [1], Sunny Chen [1], Jessica Tulloch [1] and Chang-En Yu [1,2,*]

[1] Geriatric Research, Education, and Clinical Center, VA Puget Sound Health Care System, Seattle, WA, United States of America
[2] Department of Medicine, University of Washington, Seattle, WA, United States of America
* Correspondence: Lee EG E-mail: eun-gyung.lee@va.gov; Yu CE E-mail: changeyu@uw.edu

Abstract: The *APOE* locus has garnered significant clinical interest because of its association with Alzheimer's disease (AD) and longevity. This genetic association appears across multiple genes in the *APOE* locus. Despite the apparent differences between AD and longevity, both conditions share a commonality of aging-related changes in mitochondrial function. This commonality is likely due to accumulative biological effects, partly exerted by the *APOE* locus. In this study, we investigated changes in mitochondrial structure/function-related markers using oxidative stress-induced human cellular models and postmortem brains (PMBs) from individuals with AD and normal controls. Our results reveal a range of expressional alterations, either up- or down-regulated, in these genes in response to oxidative stress. In contrast, we consistently observed an upregulation of multiple *APOE* locus genes in all cellular models and AD PMBs. Additionally, the effects of AD status on mitochondrial DNA copy number (mtDNA CN) varied depending on *APOE* genotype. Our findings imply a potential coregulation of *APOE* locus genes, possibly occurring within the same topologically associating domain (TAD) of the 3D chromosome conformation. The coordinated expression of *APOE* locus genes could impact mitochondrial function, contributing to the development of AD or longevity. Our study underscores the significant role of the *APOE* locus in modulating mitochondrial function and provides valuable insights into the underlying mechanisms of AD and aging, emphasizing the importance of this locus in clinical research.

Keywords: *APOE* locus; *TOMM40; APOE;* oxidative stress; mitochondrial dysfunction; mitochondrial DNA copy number; gene expression; Alzheimer's disease; aging

1. Introduction

The association between the *APOE* locus and AD is well established [1,2], and numerous studies have also linked this locus to longevity across diverse ethnic groups [3–7]. The genetic signals associated with AD risk or longevity in this locus cluster around four functionally distinct genes: *APOE*, *APOC1*, *NECTIN2*, and *TOMM40*. This region has also shown to contain complex genomic structures encompassing multiple regulatory elements that impact various physiologies, including cognitive health, lipid metabolism, and immunity [8–11]. Due to reduced recombination, the four genes are in strong linkage disequilibrium with e other [12,13], and genetic signals are indistinguishable between surrogates and true effectors. While *APOE* has traditionally been considered the sole effector of AD risk in this locus, the involvement of the other three genes cannot be easily dismissed. Although AD and longevity may appear to be distinct clinical manifestations, they both share the commonality of aging. AD is an aging-associated neurodegeneration, whereas longevity can be considered successful aging. One of the prominent biological features of aging is mitochondrial dysfunction, which has been extensively studied in both AD and aging [14–17]. Therefore, mitochondrial function may serve as a focal point for deciphering the true biological effects of the *APOE* locus and understanding the molecular basis of AD and longevity.

Mitochondria are dynamic organelles that constantly reshape their networks within the cell [18], influencing mitochondrial function and modifying physiology [17]. One of their distinct features is the oxidative stress response. Cells overproducing or failing to get rid of oxygen-containing free radicals, also known as reactive oxygen species (ROS), can cause oxidative stress. Excess ROS can damage DNA, RNA, lipids, and proteins, ultimately reducing cells' and tissues' performance and function and interfering with self-organizing systems and their ability to adapt to the environment [19]. Mitochondria play a crucial role in managing oxidative stress, as they are responsible for energy production, metabolic regulation, ion homeostasis, complex signaling pathways (such as stress response, immunity, and cell death). As mitochondria are the primary site for ROS generation during ATP production [20,21], defective mitochondria can become a source of excess ROS, triggering mitochondrial dysfunctions, leading to a vicious cycle [22]. Defects in mitochondrial function and dynamics, such as alterations in components, morphology, membrane potential, and mtDNA CN, can accelerate aging and contribute to AD risk [23–27].

The *APOE* locus has the potential to play a significant role in mitochondrial function. Among the four genes within the *APOE* locus, *TOMM40* has the most direct link with mitochondria. The majority of the estimated 1,500 mitochondrial proteins are encoded by nuclear genes, and these proteins are synthesized by cytosolic ribosomes and transported via the translocase of the outer membrane (TOM) complex [28]. *TOMM40* encodes TOM40 protein that creates a hydrophilic and cation-selective translocation pore of the TOM complex [29,30], functioning as a significant gateway for proteins to enter the mitochondrion [31]. Depletion of TOM40 may lead to increased levels of ROS, decreased mitochondrial integrity and ATP production, oxidative DNA damage, and mtDNA deletions [32]. Disruption of mitochondrial protein import due to Aβ blockage of TOM40 has also been proposed as a trigger for mitochondrial dysfunction in AD [33,34]. In addition to *TOMM40*, there is substantial evidence linking *APOE* with mitochondrial function. PMBs from young *APOE* ε4 carriers showed reduced cytochrome oxidase activity [35,36]. Fluorodeoxyglucose positron emission tomography studies showed decreased glucose utilization in *APOE* ε4 carriers, indicating mitochondria-related bioenergetic differences [37,38]. Furthermore, interactions between *APOE* genotypes and mtDNA haplogroups may modulate the risk of developing AD [39,40]. Due to the strong linkage disequilibrium between *APOE* and *TOMM40*, interplay between *APOE* and mitochondria may converge at the level of mitochondrial function.

Currently, there is a lack of understanding regarding the molecular mechanisms by which mitochondria impact the development of AD or longevity. The involvement of the *APOE* locus in mitochondrial function may provide valuable insights into this matter. Therefore, our study aims to investigate changes in markers and genes related to mitochondrial structure and function using human cellular models induced with oxidative stress, as well as PMBs from individuals with AD or controls. Our objective is to determine if there is a direct link between *APOE* locus genes and mitochondrial functions and to elucidate how this connection might explain the progression of AD and aging.

2. Results

2.1. Overview of the study

To investigate the role of mitochondria in the cellular response to oxidative stress, we studied three models of human brain cells: an astrocyte-like cell line (U87), a microglia-like cell line (HMC3), and a neuron-like cell line (SH-SY5Y). To induce oxidative stress, we added hydrogen peroxide (H_2O_2) to the culture media and incubated the cells for 24 hours (referred to as "c1" for the first culture condition) before measuring mitochondrial biomarkers and gene expression. To assess the cells' recovery from the H_2O_2 challenge, we replaced the treated culture media with fresh media and continued the culture for an additional 24 hr (referred to as "c2") or 48 hr (referred to as "c3") before performing various measurements. We compared the results of the treated cells to those of untreated cells. We further investigated changes in the selected cellular responses using PMB tissues to determine their relevance in AD. Table 1 provides demographic information for the PMB samples.

Preprints (www.preprints.org) | NOT PEER-REVIEWED | Posted: 28 April 2023 doi:10.20944/preprints202304.1128.v1

Table 1. Demographics of the PMB study samples

Subjects		AD	Control
Sample number_n		73	27
Gender-Female_n (%)		41 (56.2)	15 (55.6)
APOE e4_n (%)		55 (75.3)	9 (33.3)
Age at death_mean (SD)		85.88 (7.3)	88.44 (7.5)
Age at onset_mean (SD)		76.34 (9.6)	N/A
Disease Duration_mean (SD)		9.55 (4.8)	N/A
Postmortem interval_mean hour (SD)		5.06 (1.8)	5.04 (2.4)
CERAD Score			
	Absent	0	9
	Sparse	0	9
	Moderate	11	7
	Frequent	62	2
BRAAK Stage			
	I	0	5
	II	0	12
	III	0	10
	IV	0	0
	V	20	0
	VI	53	0

2.2. Oxidative stress-induced cellular responses in mitochondrial structure and function

We first evaluated the impact of oxidative stress on mitochondrial structure and function by analyzing several biomarkers, including mitochondria membrane potential (MMP), mtDNA CN, and cell viability. MMP and mtDNA CN are quantitative indicators of mitochondria structural/functional integrity, while cell viability, assessed by the MTT assay, provides a measure of stress-induced toxicity. To account for differences in viable cell numbers, we normalized MMP and mtDNA CN assays across different cell lines and experimental conditions. Detailed procedures are described in the materials and methods section. At 24 hr post-H_2O_2 treatment (c1), all three cell lines demonstrated reduced MMP (≈ 30-47%, Figure 1A), mtDNA CN (≈ 15-55%, Figure 1B), and cell viability (≈ 31-44%, Figure 1C). The glia-like cells (U87 and HMC3) exhibited a more significant reduction in mtDNA CN (>50%) than the neuron-like cell (SH-SY5Y), which had a milder reduction (≈ 15%). Similarly, SH-SY5Y showed the least reduction in MMP among the three cell lines. During the recovery phase, U87 cells restored both MMP and cell viability to their original state within 24 hr (c2), while both recoveries were much slower in HMC3 cells and were not restored to the original state even after 48 hr (c3). SH-SY5Y exhibited a MMP recovery pattern similar to those of U87 at two different recovery time points; however, its cell viability did not recover and further declined after 48 hr (≈ 80%). All cell lines' mtDNA CNs were restored to their original state after 48 hr. Our results suggest that oxidative stress immediately decreases MMP, mtDNA CN, and cell viability in all three cell types, with a more acute impact on glia-like cells. The varying degrees of impairment and restoration indicate cell-type specificity in the oxidative stress response, with astrocyte-like cells demonstrating robust mitochondrial recovery.

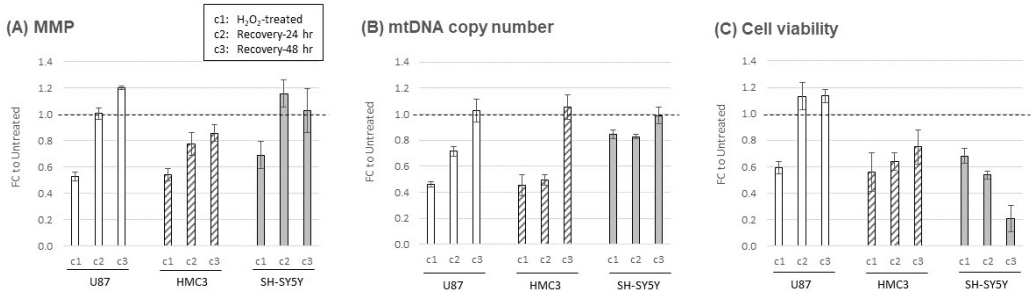

Figure 1. Oxidative stress-induced cellular responses in mitochondrial structure and function. Assays for mitochondrial membrane potential (MMP) (A), Mitochondrial DNA (mtDNA) copy

Preprints (www.preprints.org) | NOT PEER-REVIEWED | Posted: 28 April 2023 doi:10.20944/preprints202304.1128.v1

number (B), and cell viability (C) were performed on three cellular models. The fold changes (FC) of experimental conditions are compared to their untreated counterparts (set at 1.0, dashed line) and plotted as average and standard deviation of five to six independent experiments. The first culture condition, c1, represents cells treated with H_2O_2 for 24 hr; c2, cells in H_2O_2 recovery phase after replenishing culture with fresh media and continuing to culture for additional 24 hr; c3, cells in H_2O_2 recovery phase for culturing additional 48 hr.

2.3. Oxidative stress-induced alterations in mitochondrial structure and function-related gene expression

We next analyzed the expression profiles of genes associated with mitochondrial structure and functions, including antioxidant response genes (*REST*, *SOD1*, *SIRT1*), apoptotic pathway genes (*CASP3*, *CRYAB*), mitochondrial dynamics genes (*MFN1*, *FIS1*, *DNM1L*, *PINK1*), and a mtDNA maintenance gene (*TFAM*). We collected cells at 24 hr post-H_2O_2 treatment (c1) and quantified mRNA by SYBR-based RT-qPCR, comparing RNA levels to untreated controls (Figure 2). While *TFAM* expression remained unchanged across all cells, SH-SY5Y cells showed upregulation of three genes: *SOD1*, *SIRT1*, and *PINK1*. In contrast, all genes were upregulated in U87 with higher levels of antioxidant response genes (*REST*, *SOD1*) and mitochondrial dynamics genes (*MFN1*, *FIS1*). HMC3 cells showed slight up- or down-regulation, except for significantly upregulated apoptotic genes (*CASP3*, *CRYAB*). We extended the recovery phase experiment on these genes, observing that *CASP3* and *CRYAB* in HMC3 cells returned to their original state after 24-48 hr (Figure S1). The modest changes in expression levels of most genes suggest that these genes play a crucial role in mitochondrial homeostasis. Differential expression profiles suggest cell-type specificity, with astrocytes being the most sensitive to oxidative stress.

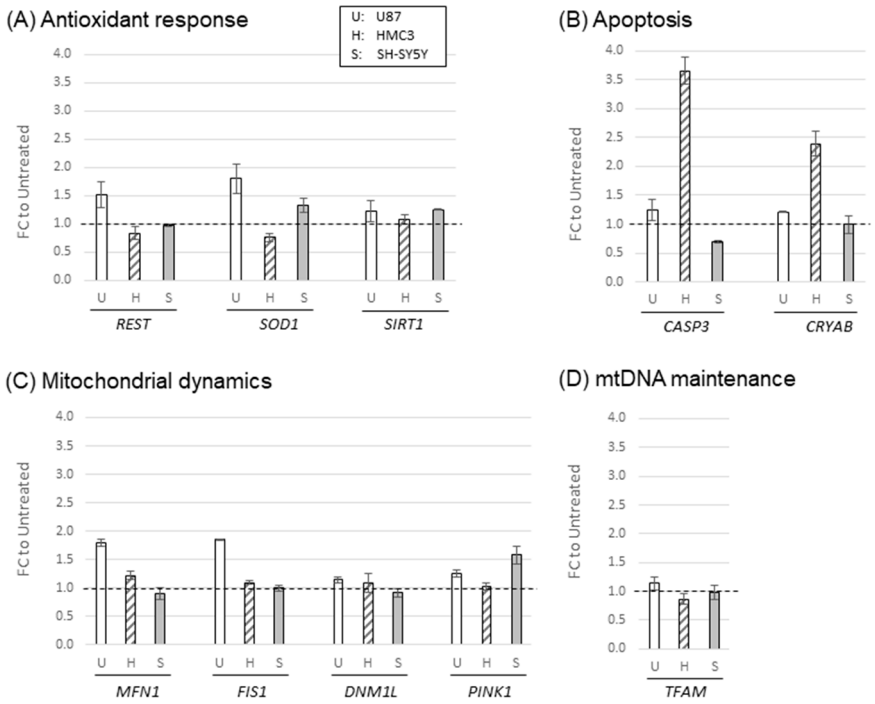

Figure 2. Oxidative stress-induced alterations in mitochondrial structure and function-related gene expression. RNA levels of three cellular models treated with H_2O_2 for 24 hr were quantified by RT-qPCR (SYBR-based). (A) Antioxidant response genes, (B) Apoptosis genes, (C) Mitochondrial dynamics genes, and (D) a mtDNA maintenance gene. The fold changes (FC) of H_2O_2-treated cells to the untreated counterpart (set at 1.0, dashed line) are plotted with average and standard deviation from three to four independent experiments.

2.4. Oxidative stress-induced alterations in APOE locus gene expression

We extended our study to explore the potential role of the *APOE* locus genes in mitochondrial function. Specifically, we examined the mRNA expression profiles of four genes located within the

Preprints (www.preprints.org) | NOT PEER-REVIEWED | Posted: 28 April 2023 doi:10.20944/preprints202304.1128.v1

APOE locus (*APOE*, *APOC1*, *NECTIN2*, and *TOMM40*) under the same experimental conditions of oxidative stress-induced cellular models. Our findings indicate that, in general, all four genes were upregulated 24 hr after H_2O_2 treatment in the three cell lines studied, except for *TOMM40* in SH-SY5Y, which showed expression level similar to its untreated counterpart (Figure 3D). Notably, the upregulation of *APOC1* was most profound in HMC3, with an approximately 50% higher expression level than U87 and SH-SY5Y (Figure 3B). During the recovery phase, the expression levels of *APOC1* and *TOMM40* gradually returned to their original state, while *NECTIN2* remained upregulated, albeit with a small decline in U87 and SH-SY5Y after 48 hr of recovery (Figure 3C). However, the expression of *APOE* was markedly different, remaining upregulated in HMC3 or continuously elevated in both U87 and SH-SY5Y as the recovery phase approached 48 hr (Figure 3A). Importantly, unlike the mitochondria structure/function-related genes we previously tested, which exhibited random profiles of either up- or down-regulation, all four *APOE* locus genes demonstrated the same trend of upregulation despite being associated with different biological pathways. This finding suggests a potential locus-specific coregulation of these *APOE* locus genes.

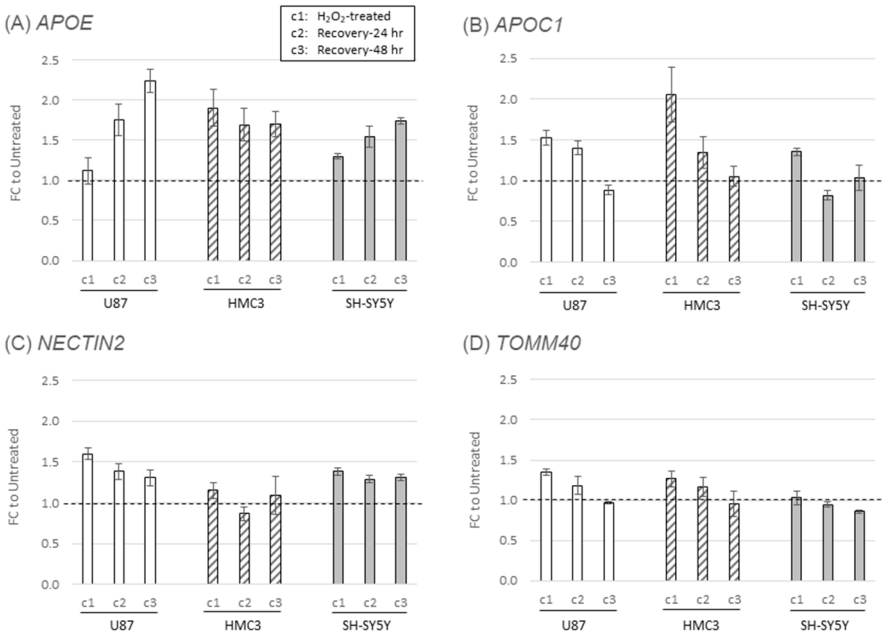

Figure 3. Alterations of *APOE* locus gene expression in response to oxidative stress. RNA levels of four genes in the *APOE* locus [*APOE* (A), *APOC1* (B), *NECTIN2* (C), and *TOMM40* (D)] in experimental conditions were measured by RT-qPCR using TaqMan assays. Fold changes (FC) to their untreated counterparts (set as baseline of 1.0) are plotted as average and standard deviation of three to four independent experiments. The first culture condition, c1, represents cells treated with H_2O_2 for 24 hr; c2, cells in H_2O_2 recovery phase after replenishing culture with fresh media and continuing to culture for additional 24 hr; c3, cells in H_2O_2 recovery phase for culturing additional 48 hr.

2.5. Mitochondrial function markers and gene expression in AD PMBs

As mitochondrial dysfunction is a key feature of AD, we sought to explore the gene expression profiles of AD PMBs to identify potential similarities with our oxidative stress-induced cellular models. Using frontal lobe tissues from AD and control subjects, we isolated total RNA and quantified mRNA levels of previously tested mitochondria-related genes. In a subset of PMB (14 AD and 10 Ctrl), we found either up- or down-regulation of these genes in AD brains (Figure S2), suggesting significant differences in mitochondria-related gene expression between AD and control brains. We also examined the expression profiles of *APOE* locus genes in the entire cohort of PMBs (73 AD and 27 Ctrl). Interestingly, all four *APOE* locus genes showed a unified pattern of upregulation in AD brains (Figure 4), suggesting a potential coregulation of these genes in response to physiological stimuli. We further quantified mtDNA CN in the entire PMB cohort without

Preprints (www.preprints.org) | NOT PEER-REVIEWED | Posted: 28 April 2023 doi:10.20944/preprints202304.1128.v1

measuring other mitochondrial markers (MMP and MTT) that require live cells. We compared mtDNA CN measures with disease status as well as SNP alleles. These SNPs include rs429358 (*APOE*), rs11568822 (*APOC1*), and rs2075650 (*TOMM40*), which all have shown strong associations with both AD and longevity. Initially, we found no significant differences when stratified by disease status (Figure 5A) or SNP alleles (Figure S3). However, there was a statistically significant interaction term between disease status and the *APOE* SNP rs429358 (p=0.027) on mtDNA CN, with the C allele (or ε4) being associated with greater mtDNA CN in AD brains (Table 2 and Figure 5B). These findings suggest that AD brains exhibit fundamental differences in mitochondrial function compared to control brains, possibly due to prolonged oxidative stress-induced mitochondrial dysfunction. Furthermore, our results suggest that the *APOE* locus may have a direct link with mitochondrial structure/function.

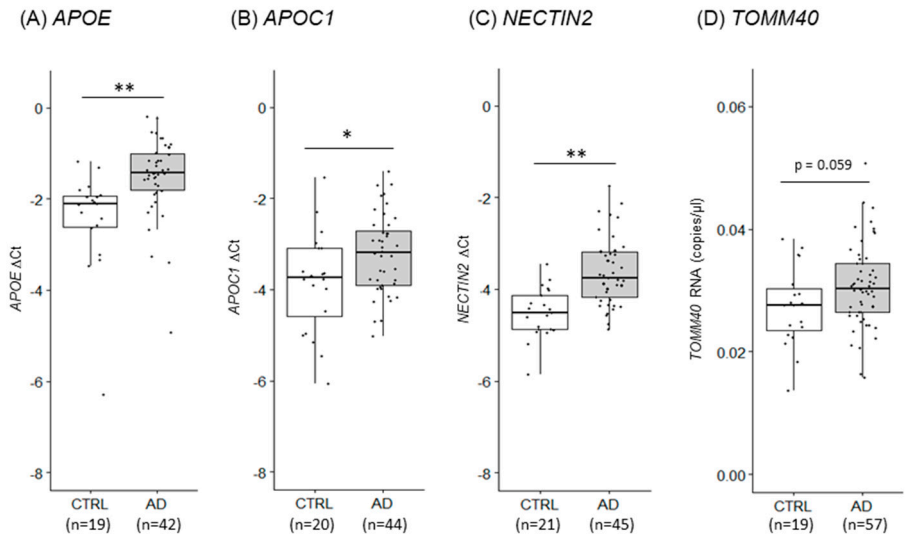

Figure 4. Variations of *APOE* locus gene expression in human PMB tissues. Using PMB samples from the AD and control (CTRL) subjects, RNA levels of four genes in the *APOE* locus were quantified by RT-qPCR (TaqMan assay): *APOE* (A), *APOC1* (B), and *NECTIN2* (C). For *TOMM40* (D), digital PCR was performed and shown as RNA copies/µl. Details are described in the methods and materials section. The ΔCt method was used: a larger ΔCt value indicates a higher RNA level. Independent samples t-test was used to compare AD and control. *, p<0.05; **, p<0.005. Numbers in parentheses denote PMB sample sizes.

Preprints (www.preprints.org) | NOT PEER-REVIEWED | Posted: 28 April 2023 doi:10.20944/preprints202304.1128.v1

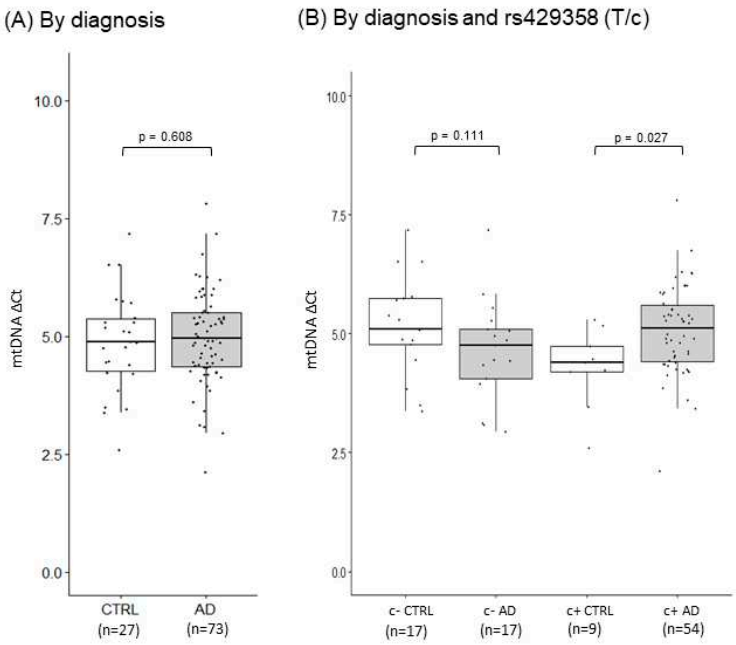

Figure 5. Human PMB mitochondrial DNA (mtDNA) copy numbers stratified by diagnosis and *APOE* genotype. Using PMB AD and control (CTRL) samples mtDNA copy numbers were quantified by RT-qPCR (SYBR-based). mtDNA copy numbers are stratified by diagnosis (A) and alleles of *APOE* SNP rs429358 (B). The normalized ΔCt shows that a larger ΔCt value indicates a greater number of mtDNA. p-values from linear mixed effects model and pairwise comparison with the covariate, *APOE* e4 status. c- indicates subjects with no e4 alleles; c+ indicates subjects with at least one e4 allele.

Table 2. Effects of SNP rs429358 in PMB mtDNA CN by a linear mixed effects model analysis

Without Covariates		
Mean (SD)		
	CTRL	4.730 (0.594)
	AD	4.855 (0.576)
Mean Difference (SE)		0.124 (0.241)
p-value		0.608
95% CI		[-0.354, 0.603]
With Covariates		
Mean (SD)		
	c- CTRL	5.178 (0.607)
	c- AD	4.643 (0.607)
	c+ CTRL	4.283 (0.646)
	c+ AD	5.067 (0.575)
Mean Difference (SE)		
	c- (CTRL vs AD)	0.535 (0.333)
p-value		0.111
95% CI		[-1.195, 0.125]
Mean Difference (SE)		
	c+ (CTRL vs AD)	0.783 (0.349)
p-value		0.027
95% CI		[0.090, 1.476]

2.6. 3D genome structure of the APOE locus

The four *APOE* locus genes are involved in different biological pathways, making it challenging to understand how they are coregulated. However, advances in chromosome conformation capture technology have enabled high-resolution mapping of chromosome architecture, providing greater insight into supranucleosomal structures such as chromatin loops and topologically associating domains (TADs). By utilizing the UCSC Genome Browser's [Hi–CandMicro–CTrackSettings(ucsc.edu)] [41,42], we identified multiple interactions among the *APOE* locus genes (Figure S4). Additionally, several independent studies have also demonstrated chromosomal interactions within this *APOE* locus [43,44]. Our findings suggest that these four *APOE* locus genes

 doi:10.20944/preprints202304.1128.v1

are located within a single TAD, creating a 3D genomic environment that facilitates their coregulation. This coregulation likely leads to a combined biological effect that can be further influenced by various factors such as epigenetics, lifestyle, environment, and age.

3. Discussion

Genetic studies have shown that the *APOE* locus contains several genes that are strongly linked to either an increased risk of AD or longevity. There are two hypotheses that could explain this observation. The first hypothesis proposes that *APOE* is the only effector and other genes' signals are surrogates due to the linkage disequilibrium property of the region. In contrast, the second hypothesis suggests that multiple genes in this locus have the combined effects that contribute to outcomes of either AD or longevity. Although the single-effector hypothesis proposes that *APOE* alone is sufficient to drive the biological consequences, given that the primary biological function of the APOE protein is in lipid metabolism, it cannot easily explain the diverse physiologies of AD or longevity. On the other hand, the multi-effector hypothesis provides a more compelling explanation, adding *APOC1* (a component of innate immunity) and *TOMM40* (a component of mitochondrial function). Despite the single-effector hypothesis dominating AD research for the last 30 years, the multi-effector hypothesis has become increasingly appealing due to advances in 3D genome technologies, which facilitates comprehension of the multiple genes' coregulation within the same locus. Since *APOE* locus is associated with AD and aging, and mitochondrial dysfunction is a common feature between AD and unsuccessful aging, we conducted this study using cellular models and PMBs to investigate the connection between the *APOE* locus and oxidative stress-related mitochondrial function. Our findings support the multi-effector hypothesis in the *APOE* locus.

Oxidative stress can induce alteration of mitochondrial markers and gene expression to alleviate cellular defects and work as a compensatory mechanism for the stress. Oxidative stress can also lead to mitochondrial dysfunction and cell death through activation of apoptotic pathway [45,46]. To investigate oxidative stress-induced changes in mitochondrial structure/function-related markers, we employed cellular models. Our data indicate that H_2O_2-induced oxidative stress immediately reduced mitochondrial membrane potential, mtDNA CN, and cell viability in all three cellular models tested. During the recovery phase, all reduced properties except cell viability in SH-SY5Y returned to their original state. This may be due to the characteristics of SH-SY5Y cell line, which includes both adherent and floating cells [47], with the latter being discarded during media changes in the recovery phase. Additionally, the mixed cell types of SH-SY5Y, including both proliferative epithelial and differentiated neuron-like cells, may also account for the decreased number of viable cells during recovery [48,49]. Among glial cells, U87 cells demonstrated the most robust recovery response, in line with the known roles of astrocytes in various structural, metabolic, and homeostatic functions in the central nervous system (CNS) [50]. In contrast, HMC3 cells showed a slower recovery rate, which may reflect the innate immunity role of microglia in transforming themselves to counter stress-induced inflammation in the CNS. Our findings suggest that the oxidative stress response exhibits robust cell-type specificity, as evidenced by varying degrees of reduction and restoration of mitochondrial function markers.

We also investigated the effects of oxidative stress on mitochondria-related gene expression. We focused on a subset of genes commonly associated with mitochondrial function and found that U87 consistently upregulated all genes during the initial oxidative stress, while HMC3 and SH-SY5Y showed mixed responses, indicating cell-specific responses to oxidative stress. In U87, the fusion/fission pathway was quickly activated, as seen by significant upregulation of genes responsible for mitochondrial fusion and fission, *MFN1* and *FIS1*. This suggests that astrocytes can quickly collaborate to address stress and maintain mitochondrial integrity. HMC3 upregulated apoptotic pathway genes, *CASP3* and *CRYAB*, to counter stress. *CRYAB* has known to be a sensitive marker for oxidative stress [51,52]; therefore, apoptosis might be one of the primary responses when microglia encountered oxidative stress in the brain. On the other hand, SH-SY5Y downregulated *CASP3*, mitigating apoptotic activation that may be beneficial for the survival of postmitotic neuron cells. SH-SY5Y also upregulated mitophagy-associated gene *PINK1*, which is a sensor for damaged

mitochondria and initiates mitophagy. This suggests that postmitotic neurons prefer mitophagy over apoptosis to maintain mitochondrial integrity. Our results show that oxidative stress causes immediate effects on mitochondrial structure and function, leading to acute changes in gene expression, which return to baseline during the recovery phase to maintain homeostasis. Cell-specific responses were also evident in this process.

Our study of the four *APOE* locus genes using cellular models yielded some surprising results. After an initial challenge of oxidative stress, we consistently observed upregulation of all four genes in all cell lines tested, which stands in stark contrast to previous experiments where we observed both up- and down-regulations of mitochondrial function-related genes. During the recovery phase, RNA levels of all upregulated *APOE* locus genes gradually returned to their untreated state, except for *APOE*. Its RNA level continued to rise even after the oxidative stress was removed, reinforcing the idea that APOE protein plays a crucial role in providing lipids that alleviate stress-induced damage as well as influencing mitochondrial biogenesis/dynamics and immunity [53,54]. Notably, we found that the RNA level of *APOE* increased the most in HMC3 cells, and the increase persisted during the recovery phase. This could be explained by *APOE*'s link in immunity. APOE is a ligand for binding to TREM2, which activates signaling pathways in microglia for cell survival, proliferation, phagocytosis, and immune responses [55,56]. Since mitochondria are a crucial component of the immune system [57], there is a natural link between mitochondria and *APOC1*. Upregulation of *APOC1* is associated with macrophage activation and possibly microglia [58], which may explain the observed upregulation of *APOC1* in HMC3 cells under oxidative stress. Furthermore, we found that *NECTIN2* remained upregulated in both U87 and SH-SY5Y cells even after a 48 hr recovery phase. *NECTIN2* encodes a single pass type I membrane glycoprotein that serves as an entry point for the herpes simplex virus and a signaling modifier in immune cell responses, indicating a potential association with mitochondria-related immune responses [59,60]. In contrast to the other three *APOE* locus genes, upregulation of *TOMM40* was observed to a much smaller extent in all three cell lines, suggesting that *TOMM40* may function as a housekeeping gene that is stably expressed and not subject to much fluctuation under different stimuli [61]. The TOM40 protein forms the main entry gate of the outer mitochondrial membrane (TOM) complex, which is responsible for the transport of all nucleus-encoded mitochondrial proteins. Therefore, genetic variants of *TOMM40* that impair transport efficiency over the long term could compromise mitochondrial function. Indeed, *TOMM40* variants have been associated with neuroinflammation and mitochondrial dysfunction, which can increase the risk of developing AD [62]. Moreover, regulatory effects of *TOMM40* variants could also affect the expression of both *TOMM40* and *APOE* [63], indicating a potential link between *TOMM40* and *APOE*. Taken together, our findings suggest that *TOMM40* may play a critical role in maintaining mitochondrial structure and function in response to oxidative stress, whereas *APOE* acts as a secondary responder with continuous upregulation to repair cellular damages. *APOC1* and *NECTIN2* may also function as secondary responders, activating the immune system to clear damaged cells or misfolded proteins in response to oxidative stress. Interestingly, all four *APOE* locus genes showed similar patterns of upregulation in all three cell lines in response to acute oxidative stress, suggesting the possibility of coregulation among these genes. This result also sheds new light on the complex interplay between *APOE* locus genes in modulating cellular responses to oxidative stress.

Our study on PMBs reveals a mixed pattern of either up- or down-regulation of mitochondria-related gene expression in AD brains when compared to control brains. In contrast, we observed a uniform upregulation of all four *APOE* locus genes in the AD brains, suggesting a potential coregulation of these genes under various physiological conditions. Moreover, our findings on mtDNA CN suggest that the progression of AD disease could affect mtDNA CN in the brain, and this effect could be modulated by the *APOE* SNP. MtDNA CN has been associated with various human diseases [64] and linked with genetic variants of the *APOE* locus [65]. Our results strengthen the rationale that multiple genes in the *APOE* locus play a direct role in mitochondrial function. As mitochondria play a crucial role in both AD and aging, their integrity and function may serve as a common intersection that mediates biological pathways and modifies physiology between the two. Damage to brain mitochondria can result in energy production deficiencies, oxidative stress, and the

 doi:10.20944/preprints202304.1128.v1

generation of mitochondria-derived damage-associated molecular patterns that trigger inflammation and neuronal damage [66,67]. Considering that mitochondrial dysfunction is a hallmark of neurodegeneration and aging, analyzing differential expression profiles and mtDNA CN between AD and control PMBs could provide valuable insights into the long-term and cumulative changes induced by oxidative stress.

Recent advances in chromosome conformation capture technology [68], including its high-throughput version (Hi-C) [69], have facilitated the high-resolution mapping of chromosomal interactions and loops that serve as the building blocks of 3D genomes. The genome is hierarchically folded and segmented into TADs [70,71]. Genes located within the same TAD region possess regulatory elements that interact with each other to form a complex gene regulatory network [72–74]. Epigenetics, lifestyle, environment, and age can modify such regulation, leading to changes in cellular states and physiology. As such, TADs can be considered the fundamental functional unit of the genome. Recently, research in AD has applied this concept [75,76]. Based on evidence from chromosome conformation capture [42–44], it is likely that multiple genes within the *APOE* locus are coregulated within the same TAD. Therefore, TADs are well-suited to study the mechanisms of coregulation of multiple genes within the *APOE* locus. Genetic variations within this region can have combined and long-term effects that modify aging-related decline in cholesterol transport (*APOE*), immunity (*APOC1*, *NECTIN2*), and mitochondrial function (*TOMM40*). With presence of suboptimal genetic variants, this locus' detrimental effect may lead to cholesterol and myelin deficiencies in CNS, impairing neuronal recovery after various damages, including infections. They may also result in the accumulation of misfolded proteins due to inadequate energy production and compromised innate immunity. Thus, genetic haplotypes variants of the *APOE* locus may either accelerate or mitigate the accumulation of brain damage with age, leading to the development of AD or successful aging.

While our study sheds light on the acute phase of the oxidative stress response and recovery, there are several limitations that warrant acknowledgement. Firstly, the cellular models we employed only captured a partial aspect of mitochondrial dynamics, and our experiments did not provide a comprehensive perspective of mitochondrial biology reflecting disease and aging due to the limited data on timing and gene pathways. Secondly, the PMB samples we collected were cross-sectional, providing only a snapshot of mitochondrial changes in the later stages of the lifespan. Therefore, our findings may not fully represent the entire process of mitochondrial dysfunction during aging and disease. Addressing these limitations would require further studies that utilize longitudinal data with larger sample sizes to provide a more comprehensive understanding of mitochondrial biology in the context of aging and disease.

4. Materials and Methods

4.1. Human PMB and cell lines

Human biospecimen were obtained from the University of Washington (UW) Alzheimer's Disease Research Center after approval by the institutional review board of the Veterans Affairs Puget Sound Health Care System (MIRB# 00331). Since the human specimens have already been collected by other established programs, no consent was obtained for this work. AD patient diagnosis was confirmed postmortem by neuropathological analysis. Clinically normal subjects were volunteers over 65 years of age, never diagnosed with AD, and lacked AD neuropathology at autopsy. Demographics of the PMB samples are listed in Table 1. Postmortem frontal lobe tissues were obtained from the middle frontal gyrus tissues that were rapidly frozen at autopsy (<10 hours after death) and stored at –80˚C until use. Glioblastoma U87 MG cells (ATCC) grew in 89% Dulbecco's modified Eagle's medium (DMEM) (Gibco); Microglia HMC3 cells (ATCC) were grown in 89% Eagle's Minimum Essential Medium (EMEM) (ATCC); neuroblastoma SH-SY5Y cells (ATCC) were grown in 89% DMEM with F12. All these media were supplemented with 1% penicillin/ streptomycin and cells cultured at 37˚C in a 5% CO_2 atmosphere.

 doi:10.20944/preprints202304.1128.v1

4.2. Hydrogen Peroxide Treatment

Twenty-four hours prior to treatment, three cell lines (U87, HMC3 and SH-SY5Y) were seeded at a density of 70-80%. For the assays of mtDNA CN and gene expression, cells were seeded on a 6-well plate, while a 96-well plate was used for mitochondrial membrane potential assay and cell viability assay. The optimal concentration of hydrogen peroxide, H_2O_2 (Sigma), for each cell line was determined when over 70-80% cells remained healthy during 24 hr treatment. 600 μM (U87), 400 μM (HMC3), or 100 μM (SH-SY5Y) H_2O_2 was added to the cell culture and incubated for 24 hr at 37°C, 5% CO_2 (designated "c1" for the first culture condition). Also, cells were assayed during recovery phase of H_2O_2-induced oxidative stress. To do this, cells were treated with H_2O_2 for 24 hr and cell media was replenished with fresh growth media and cells were incubated for 24 hr (designated "c2") or 48 hr (designated "c3"). For each condition, we set up the control without treatment and compared it with treated conditions. The treated and untreated cells were collected and subjected to genomic DNA and total RNA isolation. Three to four independent experiments were performed.

4.3. DNA/RNA extraction

Genomic DNA and RNA were isolated from cultured cell lines and frozen PMB tissues from the frontal cortex. Genomic DNA was extracted using the QIAmp DNA Blood Mini Kit (Qiagen) and RNA was extracted using AllPrep DNA/RNA Mini Kit (Qiagen) according to the manufacturer's protocols. Nucleic acid concentrations were measured by NanoPhotometer (Implen), and samples were stored at –20°C prior to use.

4.4. Mitochondrial membrane potential (MMP) assay

MMP of the human cell lines was measured using a MitoProbe JC-1 assay kit (ThermoFisher). The cationic dye, JC-1 (5′,6,6′-tetrachloro-1,1′,3,3′-tetraethylbenzimidazolylcarbocyanine iodide), exhibits membrane potential-dependent accumulation in mitochondria, which is indicated by a fluorescence emission shift from monomeric green (529 nm) to JC-1 aggregates red (590 nm). Consequently, MMP change in response to cellular stimuli is represented by the ratio of red to green fluorescence intensity. This ratio of red dye aggregated in mitochondria to monomeric green dye was used to account for variations in total number of viable cells in experimental conditions. The membrane potential disrupter, CCCP (carbonyl cyanide 3-cholorophenylhydrazone), was included in all assays as a control. 24 hr prior to H_2O_2 treatment, cells were seeded at a density of 70-80% on a 96-well black plate with clear bottom. The seeded cells were treated with H_2O_2 for 24 hr, and then proceeded to MMP assay. After washing cells on the plate with growth media, 2 μM JC-1 was added and incubated at 37ºC, 5% CO_2 for 30 min. The reaction plate was washed with PBS and fluorescence was measured in 488 nm excitation and green (529 nm) or red (590 nm) emission using SpectraMax M2 plate reader (Molecular Devices). All procedures were performed according to the manufacturers' protocols. MMP fold change (FC) of H_2O_2-treated to untreated was computed as FC (treated) = MMP (treated)/MMP (untreated). Five to six independent experiments were performed.

4.5. Mitochondrial DNA copy number (mtDNA CN) assay

MtDNA CN was quantitated by SYBR-based quantitative PCR (qPCR). Mitochondria-encoded NADH dehydrogenase 1 (*MT-ND1*) copy numbers were quantitated and normalized by copy numbers of a single copy reference gene, nuclear receptor coactivator 3 (*NCOA3*). Reactions for *MT-ND1* and *NCOA3* were run separately in a 384 well optical plate in triplicate using QuantStudio 5 (ThermoFisher). Since there are so many copies of mtDNA compared to the single copy reference gene, optimal amounts of genomic DNA need to be determined by that cycle threshold (Ct) is in the linear range of the amplification curve. 0.1 ng of genomic DNA for *MT-ND1* and 3.3 ng for *NCOA3* were used in qPCR assays. As a constant amount of input DNA was used for mtDNA CN measurement, variations in total number of viable cells were taken into account when analyzed in experimental conditions. The 10 μl reaction included respective amounts of DNA for *MT-ND1* or *NCOA3*, 5 μl of Power SYBR GREEN PCR Master Mix (Applied Biosystems, ThermoFisher), and 0.5

μM of each forward and reverse primer. Thermal cycling profile consisted of 2 minutes at 50°C, 10 minutes at 95°C, and then 40 cycles of 15 seconds at 95°C, 60 seconds at 56°C, and 60 seconds at 72°C. ΔCt method was used to control for the quantity of input DNA by the single copy reference gene *NCOA3*. The normalized ΔCt = mean of *NCOA3* Ct triplicate–Ct (*MT-ND1*). In this setting, a larger ΔCt value indicates a higher mtDNA CN. Also, fold change of H_2O_2-treated to untreated was computed as FC (treated) = $2^{-\Delta\Delta Ct}$, where ΔΔCt = ΔCt (treated)–ΔCt (untreated).

4.6. Cell viability assay

MTT (3-(4,5-dimethylthiazol-2-yl)-2,5-diphenyltetrazolium bromide) assay was performed for measuring cell viability, cell proliferation and cytotoxicity. This assay is based on the conversion of water soluble MTT compound to an insoluble formazan by metabolically active cells, resulting in color formation at OD590 nm. Dead cells lose this ability and show no signal. The measured absorbance at OD590 nm is proportional to the number of viable cells. FC (treated) = OD590 (treated)/OD590 (untreated).

4.7. Gene expression by reverse transcriptase (RT) reaction and quantitative PCR (qPCR) assay

Total RNA (100 ng) was used for each 20 μl RT reaction, and cDNA synthesis was performed using the PrimeScript RT Reagent Kit (Takara Bio USA). The resulting cDNA was diluted 20 times for qPCR, and expression levels were measured using TaqMan assays in a QuantStudio 5 (ThermoFisher). Each 10 μl qPCR reaction contained a fixed RNA input (5 ng), 0.5 μl of the 20x TaqMan assay, and 5 μl of 2x TaqMan Universal PCR Reaction Mix (Applied Biosystems, Thermo Fisher). The thermal cycling program consisted of 2 minutes at 50°C, 10 minutes at 95°C, and then 40 cycles of 15 seconds at 95°C and 1 minute at 60°C. For mitochondrial structure and function-related gene expression, SYBR PCR reactions were run on a QuantStudio 5 (ThermoFisher) with the same thermal cycling program as used for the TaqMan assays. Triplicate qPCR assays were performed for all gene expression experiments. To control for the quantity of input RNA, we quantified *ACTB* mRNA as an internal control for each sample and obtained a normalized ΔCt value: mean of the *ACTB* Ct triplicate - Ct (target). In this setting, ΔCt values were near or below zero, as *ACTB* mRNA levels were higher than those of target genes; a larger ΔCt value indicates a higher RNA level. Additionally, fold change of H_2O_2-treated to untreated was computed as FC (treated) = $2^{-\Delta\Delta Ct}$, where ΔΔCt = ΔCt (treated)–ΔCt (untreated). Information on primers, probes and TaqMan assays is listed in Table S1.

4.8. TOMM40 allelic gene expression

For measurement of *TOMM40* RNA level in PMB sample, quantification of allelic gene expression was performed by pyrosequencing combined with duplex digital PCR. Previously, we have shown that commercial TaqMan assay was not suitable for accurate measurement of *TOMM40* RNA, likely due to the presence of *TOMM40* pseudogenes RNA [11]. For *TOMM40* allelic gene expression assay, first, a DNA segment of *TOMM40* spanning exon 3 and exon 4 was PCR-amplified using a biotinylated forward primer and a reverse primer in which the strand to serve as the pyrosequencing template is biotinylated. After denaturation, the biotinylated single-stranded PCR amplicon was subjected to hybridize with a sequencing primer. The pyrogram signal peak for the *TOMM40*-specific allele distinct from *TOMM40* pseudogene allele was represented as percentage. Pyrosequencing was carried out on a PyroMark Q24 system (Qiagen) and data were analyzed using PyroMark Q24 software, version 2.0.6 (Qiagen). Then, the copy number of *TOMM40* total RNA including *TOMM40* pseudogene RNA was quantified by a duplex digital PCR. Two pairs of primer and probe mix corresponding to *TOMM40* and *ACTB* were run together in a reaction using QIAcuity dPCR (Qiagen). All procedures were performed according to the manufacturers' protocols. Using *ACTB* as an endogenous control, the *TOMM40* RNA copy number was normalized by *ACTB* RNA copy number. The final computed *TOMM40* RNA copy number: the normalized *TOMM40* RNA copy

 doi:10.20944/preprints202304.1128.v1

number x the percentage of the *TOMM40* allele. Information on primers, probes and TaqMan assays is listed in Table S1.

4.9. Genotyping of APOE, TOMM40 and APOC1

Genomic DNA isolated from frozen PMB samples was used for genotyping. The ε2/ε3/ε4 alleles of *APOE* single nucleotide polymorphism (SNP), rs429358, were genotyped using two TaqMan allele discrimination assays (C_3084793_20 and C_904973_10, ThermoFisher). The *TOMM40* SNP, rs2075650, was genotyped using TaqMan allele discrimination assays (C_3084828_20 and C_31478296_10, ThermoFisher). The *APOC1* SNP, rs11568822 (In/del), was genotyped by restriction fragment length polymorphism (RFLP). A small fragment enclosing the *APOC1* SNP region was amplified by standard Hot Start PCR with a primer pair: Ch19_50109453F (5′ - ATTCCCCGAACGAATAAACC - 3′) and Ch19_50109512R (5′ - AGCCGCAGACAAAATTCCT - 3′). The PCR fragment was digested with the enzyme HpaI (cut site GTT^AAC) and analyzed for the fragment size difference between insertion (CGTT) and deletion using QIAxcel with DNA High Resolution Cartridge (Qiagen).

4.10. Statistical analysis and box plot

The figures were created using the software R-Program Version R-4.2.2 for Windows. The package ggpubr (CRAN - Package ggpubr (r-project.org)) was used to generate the box plots. The package rstatix (CRAN - Package rstatix (r-project.org)) was used to perform independent samples t-test. Statistical analyses including linear mixed effects model and pairwise comparison were performed on IBM SPSS Statistics 19 for Windows, Version 19.0 (IBM Corp.).

5. Conclusions

The *APOE* locus harbors several genes that could be coregulated. Among these genes, *APOE* participates in lipid transport and clearance of neuropathological aggregates, *APOC1* and *NECTIN2* regulate innate immunity, and *TOMM40* facilitates mitochondrial protein transport. These genes are most likely located within the same TAD of the 3D chromosome conformation, enabling an efficient coregulatory response to environmental cues and insults, particularly when the locus genes are involved in multiple pathways. The collective impact of these genes could modulate mitochondrial biology, ultimately leading to either the development of AD or a path towards healthy aging.

Supplementary Materials: The following supporting information can be downloaded at the website of this paper posted on Preprints.org. Figure S1: Alterations of apoptosis-related gene expression during the H_2O_2 recovery phase; Figure S2: Variations of mitochondrial structure and function-related gene expression in human PMB tissues; Figure S3: Variations of mitochondrial DNA (mtDNA) copy numbers in human PMB tissues; Figure S4: Three-dimensional genome structure of the *APOE* locus; Table S1: Primers, probes and TaqMan assays

Author Contributions: Conceptualization, EGL, CEY; methodology, EGL, CEY, LL, SC; formal analysis, EGL, SC, JT; resources, CEY, EGL, LL; Data curation, EGL, SC; writing-original draft preparation, CEY; writing-review and editing, EGL, JT; visualization, EGL, CEY, SC; supervision, EGL, CEY; project administration, CEY; funding acquisition, CEY. All authors have read and agreed to the published version of the manuscript.

Funding: This research was funded by Merit Review Awards, BX000933 and BX004823, from the U.S. Department of Veterans Affairs Office of Research and Development Biomedical Laboratory Research Program. The contents do not represent the views of the U.S. Department of Veterans Affairs or the United States Government.

Institutional Review Board Statement: This study was conducted according to the guidelines of the the Veterans Affairs Puget Sound Health Care System (MIRB# 00331).

Data Availability Statement: the data presented in this study are available on request from the corresponding authors.

Conflicts of Interest: The authors declare no conflict of interest.

References

1. Lambert JC, Ibrahim-Verbaas CA, Harold D, Naj AC, Sims R, Bellenguez C, et al. Meta-analysis of 74,046 individuals identifies 11 new susceptibility loci for Alzheimer's disease. Nat Genet. 2013;45(12):1452-8. doi: 10.1038/ng.2802. PubMed PMID: 24162737; PubMed Central PMCID: PMCPMC3896259.
2. Beecham GW, Hamilton K, Naj AC, Martin ER, Huentelman M, Myers AJ, et al. Genome-wide association meta-analysis of neuropathologic features of Alzheimer's disease and related dementias. PLoS Genet. 2014;10(9):e1004606. doi: 10.1371/journal.pgen.1004606. PubMed PMID: 25188341; PubMed Central PMCID: PMCPMC4154667.
3. Nebel A, Kleindorp R, Caliebe A, Nothnagel M, Blanche H, Junge O, et al. A genome-wide association study confirms APOE as the major gene influencing survival in long-lived individuals. Mech Ageing Dev. 2011;132(6-7):324-30. doi: 10.1016/j.mad.2011.06.008. PubMed PMID: 21740922.
4. Lin R, Zhang Y, Yan D, Liao X, Gong G, Hu J, et al. Association of common variants in TOMM40/APOE/APOC1 region with human longevity in a Chinese population. J Hum Genet. 2016;61(4):323-8. doi: 10.1038/jhg.2015.150. PubMed PMID: 26657933.
5. Yashin AI, Arbeev KG, Wu D, Arbeeva LS, Bagley O, Stallard E, et al. Genetics of Human Longevity From Incomplete Data: New Findings From the Long Life Family Study. J Gerontol A Biol Sci Med Sci. 2018;73(11):1472-81. doi: 10.1093/gerona/gly057. PubMed PMID: 30299504; PubMed Central PMCID: PMCPMC6175028
6. Deelen J, Evans DS, Arking DE, Tesi N, Nygaard M, Liu X, et al. A meta-analysis of genome-wide association studies identifies multiple longevity genes. Nat Commun. 2019;10(1):3669. doi: 10.1038/s41467-019-11558-2. PubMed PMID: 31413261; PubMed Central PMCID: PMCPMC6694136.
7. Kulminski AM, Jain-Washburn E, Philipp I, He L, Loika Y, Loiko E, et al. APOE varepsilon4 allele and TOMM40-APOC1 variants jointly contribute to survival to older ages. Aging Cell. 2022:e13730. doi: 10.1111/acel.13730. PubMed PMID: 36330582.
8. Bekris LM, Lutz F, Yu CE. Functional analysis of APOE locus genetic variation implicates regional enhancers in the regulation of both TOMM40 and APOE. J Hum Genet. 2012;57(1):18-25. Epub 2011/11/18. doi: 10.1038/jhg.2011.123. PubMed PMID: 22089642; PubMed Central PMCID: PMCPMC3266441.
9. Fuior EV, Gafencu AV. Apolipoprotein C1: Its Pleiotropic Effects in Lipid Metabolism and Beyond. Int J Mol Sci. 2019;20(23). doi: 10.3390/ijms20235939. PubMed PMID: 31779116; PubMed Central PMCID: PMCPMC6928722.
10. Heinemeyer T, Stemmet M, Bardien S, Neethling A. Underappreciated Roles of the Translocase of the Outer and Inner Mitochondrial Membrane Protein Complexes in Human Disease. DNA Cell Biol. 2019;38(1):23-40. doi: 10.1089/dna.2018.4292. PubMed PMID: 30481057.
11. Lee EG, Chen S, Leong L, Tulloch J, Yu CE. TOMM40 RNA Transcription in Alzheimer's Disease Brain and Its Implication in Mitochondrial Dysfunction. Genes (Basel). 2021;12(6). doi: 10.3390/genes12060871. PubMed PMID: 34204109; PubMed Central PMCID: PMCPMC8226536.
12. Yu CE, Seltman H, Peskind ER, Galloway N, Zhou PX, Rosenthal E, et al. Comprehensive analysis of APOE and selected proximate markers for late-onset Alzheimer's disease: patterns of linkage disequilibrium and disease/marker association. Genomics. 2007;89(6):655-65. doi: 10.1016/j.ygeno.2007.02.002. PubMed PMID: 17434289; PubMed Central PMCID: PMCPMC1978251.
13. Roses A, Sundseth S, Saunders A, Gottschalk W, Burns D, Lutz M. Understanding the genetics of APOE and TOMM40 and role of mitochondrial structure and function in clinical pharmacology of Alzheimer's disease. Alzheimers Dement. 2016;12(6):687-94. doi: 10.1016/j.jalz.2016.03.015. PubMed PMID: 27154058.
14. Kujoth GC, Hiona A, Pugh TD, Someya S, Panzer K, Wohlgemuth SE, et al. Mitochondrial DNA mutations, oxidative stress, and apoptosis in mammalian aging. Science. 2005;309(5733):481-4. doi: 10.1126/science.1112125. PubMed PMID: 16020738.
15. Zafrilla P, Mulero J, Xandri JM, Santo E, Caravaca G, Morillas JM. Oxidative stress in Alzheimer patients in different stages of the disease. Curr Med Chem. 2006;13(9):1075-83. doi: 10.2174/092986706776360978. PubMed PMID: 16611085.
16. Liguori I, Russo G, Curcio F, Bulli G, Aran L, Della-Morte D, et al. Oxidative stress, aging, and diseases. Clin Interv Aging. 2018;13:757-72. doi: 10.2147/CIA.S158513. PubMed PMID: 29731617; PubMed Central PMCID: PMCPMC5927356.
17. Swerdlow RH. The Alzheimer's Disease Mitochondrial Cascade Hypothesis: A Current Overview. J Alzheimers Dis. 2023. doi: 10.3233/JAD-221286. PubMed PMID: 36806512.

18. Bereiter-Hahn J, Jendrach M. Mitochondrial dynamics. Int Rev Cell Mol Biol. 2010;284:1-65. doi: 10.1016/S1937-6448(10)84001-8. PubMed PMID: 20875628.
19. Juan CA, Perez de la Lastra JM, Plou FJ, Perez-Lebena E. The Chemistry of Reactive Oxygen Species (ROS) Revisited: Outlining Their Role in Biological Macromolecules (DNA, Lipids and Proteins) and Induced Pathologies. Int J Mol Sci. 2021;22(9). doi: 10.3390/ijms22094642. PubMed PMID: 33924958; PubMed Central PMCID: PMCPMC8125527.
20. Verri M, Pastoris O, Dossena M, Aquilani R, Guerriero F, Cuzzoni G, et al. Mitochondrial alterations, oxidative stress and neuroinflammation in Alzheimer's disease. Int J Immunopathol Pharmacol. 2012;25(2):345-53. doi: 10.1177/039463201202500204. PubMed PMID: 22697066.
21. Flannery PJ, Trushina E. Mitochondrial dynamics and transport in Alzheimer's disease. Mol Cell Neurosci. 2019;98:109-20. doi: 10.1016/j.mcn.2019.06.009. PubMed PMID: 31216425; PubMed Central PMCID: PMCPMC6614006.
22. Butterfield DA, Halliwell B. Oxidative stress, dysfunctional glucose metabolism and Alzheimer disease. Nat Rev Neurosci. 2019;20(3):148-60. doi: 10.1038/s41583-019-0132-6. PubMed PMID: 30737462; PubMed Central PMCID: PMCPMC9382875.
23. Hirai K, Aliev G, Nunomura A, Fujioka H, Russell RL, Atwood CS, et al. Mitochondrial abnormalities in Alzheimer's disease. J Neurosci. 2001;21(9):3017-23. doi: 10.1523/JNEUROSCI.21-09-03017.2001. PubMed PMID: 11312286; PubMed Central PMCID: PMCPMC6762571.
24. Kwong JQ, Beal MF, Manfredi G. The role of mitochondria in inherited neurodegenerative diseases. J Neurochem. 2006;97(6):1659-75. doi: 10.1111/j.1471-4159.2006.03990.x. PubMed PMID: 16805775.
25. Wang X, Su B, Zheng L, Perry G, Smith MA, Zhu X. The role of abnormal mitochondrial dynamics in the pathogenesis of Alzheimer's disease. J Neurochem. 2009;109 Suppl 1(Suppl 1):153-9. doi: 10.1111/j.1471-4159.2009.05867.x. PubMed PMID: 19393022; PubMed Central PMCID: PMCPMC2720030.
26. Kapogiannis D, Mattson MP. Disrupted energy metabolism and neuronal circuit dysfunction in cognitive impairment and Alzheimer's disease. Lancet Neurol. 2011;10(2):187-98. doi: 10.1016/S1474-4422(10)70277-5. PubMed PMID: 21147038; PubMed Central PMCID: PMCPMC3026092.
27. Swerdlow RH, Burns JM, Khan SM. The Alzheimer's disease mitochondrial cascade hypothesis: progress and perspectives. Biochim Biophys Acta. 2014;1842(8):1219-31. doi: 10.1016/j.bbadis.2013.09.010. PubMed PMID: 24071439; PubMed Central PMCID:PMCPMC3962811.
28. Hoogenraad NJ, Ward LA, Ryan MT. Import and assembly of proteins into mitochondria of mammalian cells. Biochim Biophys Acta. 2002;1592(1):97-105. Epub 2002/08/23. doi: S0167488902002689 [pii]. PubMed PMID: 12191772.
29. Hill K, Model K, Ryan MT, Dietmeier K, Martin F, Wagner R, et al. Tom40 forms the hydrophilic channel of the mitochondrial import pore for preproteins [see comment]. Nature. 1998;395(6701):516-21. doi: 10.1038/26780. PubMed PMID: 9774109.
30. Suzuki H, Okazawa Y, Komiya T, Saeki K, Mekada E, Kitada S, et al. Characterization of rat TOM40, a central component of the preprotein translocase of the mitochondrial outer membrane. J Biol Chem. 2000;275(48):37930-6. doi: 10.1074/jbc.M006558200. PubMed PMID: 10980201.
31. Chacinska A, Koehler CM, Milenkovic D, Lithgow T, Pfanner N. Importing mitochondrial proteins: machineries and mechanisms. Cell. 2009;138(4):628-44. doi: 10.1016/j.cell.2009.08.005. PubMed PMID: 19703392; PubMed Central PMCID: PMCPMC4099469.
32. Bender A, Desplats P, Spencer B, Rockenstein E, Adame A, Elstner M, et al. TOM40 mediates mitochondrial dysfunction induced by alpha-synuclein accumulation in Parkinson's disease. PLoS One. 2013;8(4):e62277. doi: 10.1371/journal.pone.0062277. PubMed PMID: 23626796; PubMed Central PMCID: PMCPMC3633917.
33. Anandatheerthavarada HK, Devi L. Mitochondrial translocation of amyloid precursor protein and its cleaved products: relevance to mitochondrial dysfunction in Alzheimer's disease. Rev Neurosci. 2007;18(5):343-54. doi: 10.1515/revneuro.2007.18.5.343. PubMed PMID: 19544621.
34. Cenini G, Rub C, Bruderek M, Voos W. Amyloid beta-peptides interfere with mitochondrial preprotein import competence by a coaggregation process. Mol Biol Cell. 2016;27(21):3257-72. doi: 10.1091/mbc.E16-05-0313. PubMed PMID: 27630262; PubMed Central PMCID: PMCPMC5170859.
35. Perkins M, Wolf AB, Chavira B, Shonebarger D, Meckel JP, Leung L, et al. Altered Energy Metabolism Pathways in the Posterior Cingulate in Young Adult Apolipoprotein E varepsilon4 Carriers. J Alzheimers Dis. 2016;53(1):95-106. doi: 10.3233/JAD-151205. PubMed PMID: 27128370; PubMed Central PMCID: PMCPMC4942726.

36. Valla J, Yaari R, Wolf AB, Kusne Y, Beach TG, Roher AE, et al. Reduced posterior cingulate mitochondrial activity in expired young adult carriers of the APOE epsilon4 allele, the major late-onset Alzheimer's susceptibility gene. J Alzheimers Dis. 2010;22(1):307-13. doi: 10.3233/JAD-2010-100129. PubMed PMID: 20847408; PubMed Central PMCID: PMCPMC3124564.
37. Reiman EM, Caselli RJ, Yun LS, Chen K, Bandy D, Minoshima S, et al. Preclinical evidence of Alzheimer's disease in persons homozygous for the epsilon 4 allele for apolipoprotein E. N Engl J Med. 1996;334(12):752-8. doi: 10.1056/NEJM199603213341202. PubMed PMID: 8592548.
38. Small GW, Mazziotta JC, Collins MT, Baxter LR, Phelps ME, Mandelkern MA, et al. Apolipoprotein E type 4 allele and cerebral glucose metabolism in relatives at risk for familial Alzheimer disease. JAMA. 1995;273(12):942-7. PubMed PMID: 7884953.
39. Carrieri G, Bonafe M, De Luca M, Rose G, Varcasia O, Bruni A, et al. Mitochondrial DNA haplogroups and APOE4 allele are non-independent variables in sporadic Alzheimer's disease. Hum Genet. 2001;108(3):194-8. PubMed PMID: 11354629.
40. Maruszak A, Canter JA, Styczynska M, Zekanowski C, Barcikowska M. Mitochondrial haplogroup H and Alzheimer's disease--is there a connection? Neurobiol Aging. 2009;30(11):1749-55. doi: 10.1016/j.neurobiolaging.2008.01.004. PubMed PMID: 18308428.
41. Hsieh TS, Fudenberg G, Goloborodko A, Rando OJ. Micro-C XL: assaying chromosome conformation from the nucleosome to the entire genome. Nat Methods. 2016;13(12):1009-11. doi: 10.1038/nmeth.4025. PubMed PMID: 27723753.
42. Krietenstein N, Abraham S, Venev SV, Abdennur N, Gibcus J, Hsieh TS, et al. Ultrastructural Details of Mammalian Chromosome Architecture. Mol Cell. 2020;78(3):554-65 e7. doi: 10.1016/j.molcel.2020.03.003. PubMed PMID: 32213324; PubMed Central PMCID: PMCPMC7222625.
43. Nuytemans K, Lipkin Vasquez M, Wang L, Van Booven D, Griswold AJ, Rajabli F, et al. Identifying differential regulatory control of APOE varepsilon4 on African versus European haplotypes as potential therapeutic targets. Alzheimers Dement. 2022;18(10):1930-42. doi: 10.1002/alz.12534. PubMed PMID: 34978147; PubMed Central PMCID: PMCPMC9250552.
44. Meng G, Xu H, Lu D, Li S, Zhao Z, Li H, et al. Three-dimensional chromatin architecture datasets for aging and Alzheimer's disease. Sci Data. 2023;10(1):51. doi: 10.1038/s41597-023-01948-z. PubMed PMID: 36693875; PubMed Central PMCID: PMCPMC9873630.
45. Periasamy A, Mitchell N, Zaytseva O, Chahal AS, Zhao J, Colman PM, et al. An increase in mitochondrial TOM activates apoptosis to drive retinal neurodegeneration. Sci Rep. 2022;12(1):21634. doi: 10.1038/s41598-022-23280-z. PubMed PMID: 36517509; PubMed Central PMCID: PMCPMC9750964.
46. Shao D, Gao Z, Zhao Y, Fan M, Zhao X, Wei Q, et al. Sulforaphane Suppresses H(2)O(2)-Induced Oxidative Stress and Apoptosis via the Activation of AMPK/NFE2L2 Signaling Pathway in Goat Mammary Epithelial Cells. Int J Mol Sci. 2023;24(2). doi: 10.3390/ijms24021070. PubMed PMID: 36674585; PubMed Central PMCID: PMCPMC9867344.
47. Kovalevich J, Santerre M, Langford D. Considerations for the Use of SH-SY5Y Neuroblastoma Cells in Neurobiology. Methods Mol Biol. 2021;2311:9-23. doi: 10.1007/978-1-0716-1437-2_2. PubMed PMID: 34033074.
48. Pratiwi R, Nantasenamat C, Ruankham W, Suwanjang W, Prachayasittikul V, Prachayasittikul S, et al. Mechanisms and Neuroprotective Activities of Stigmasterol Against Oxidative Stress-Induced Neuronal Cell Death via Sirtuin Family. Front Nutr. 2021;8:648995. doi: 10.3389/fnut.2021.648995. PubMed PMID: 34055852; PubMed Central PMCID: PMCPMC8149742.
49. Lingappa S, Shivakumar MS, Manivasagam T, Somasundaram ST, Seedevi P. Neuroprotective Effect of Epalrestat on Hydrogen Peroxide-Induced Neurodegeneration in SH-SY5Y Cellular Model. J Microbiol Biotechnol. 2021;31(6):867-74. doi: 10.4014/jmb.2101.01002. PubMed PMID: 33820886; PubMed Central PMCID: PMCPMC9705952.
50. Santello M, Toni N, Volterra A. Astrocyte function from information processing to cognition and cognitive impairment. Nat Neurosci. 2019;22(2):154-66. doi: 10.1038/s41593-018-0325-8. PubMed PMID: 30664773.
51. Kamradt MC, Chen F, Cryns VL. The small heat shock protein alpha B-crystallin negatively regulates cytochrome c- and caspase-8-dependent activation of caspase-3 by inhibiting its autoproteolytic maturation. J Biol Chem. 2001;276(19):16059-63. doi: 10.1074/jbc.C100107200. PubMed PMID: 11274139.

52. Morrow G, Samson M, Michaud S, Tanguay RM. Overexpression of the small mitochondrial Hsp22 extends Drosophila life span and increases resistance to oxidative stress. FASEB J. 2004;18(3):598-9. doi: 10.1096/fj.03-0860fje. PubMed PMID: 14734639.
53. Yin J, Reiman EM, Beach TG, Serrano GE, Sabbagh MN, Nielsen M, et al. Effect of ApoE isoforms on mitochondria in Alzheimer disease. Neurology. 2020;94(23):e2404-e11. doi: 10.1212/WNL.0000000000009582. PubMed PMID: 32457210; PubMed Central PMCID: PMCPMC7455369.
54. Kloske CM, Barnum CJ, Batista AF, Bradshaw EM, Brickman AM, Bu G, et al. APOE and immunity: Research highlights. Alzheimers Dement. 2023. doi: 10.1002/alz.13020. PubMed PMID: 36975090.
55. Wolfe CM, Fitz NF, Nam KN, Lefterov I, Koldamova R. The Role of APOE and TREM2 in Alzheimer's Disease-Current Understanding and Perspectives. Int J Mol Sci. 2018;20(1). doi: 10.3390/ijms20010081. PubMed PMID: 30587772; PubMed Central PMCID: PMCPMC6337314.
56. Gratuze M, Leyns CEG, Holtzman DM. New insights into the role of TREM2 in Alzheimer's disease. Mol Neurodegener. 2018;13(1):66. doi: 10.1186/s13024-018-0298-9. PubMed PMID: 30572908; PubMed Central PMCID: PMCPMC6302500.
57. Mills EL, Kelly B, O'Neill LAJ. Mitochondria are the powerhouses of immunity. Nat Immunol. 2017;18(5):488-98. doi: 10.1038/ni.3704. PubMed PMID: 28418387.
58. Wilson JL, Mayr HK, Weichhart T. Metabolic Programming of Macrophages: Implications in the Pathogenesis of Granulomatous Disease. Front Immunol. 2019;10:2265. doi: 10.3389/fimmu.2019.02265. PubMed PMID: 31681260; PubMed Central PMCID: PMCPMC6797840.
59. Wu B, Zhong C, Lang Q, Liang Z, Zhang Y, Zhao X, et al. Poliovirus receptor (PVR)-like protein cosignaling network: new opportunities for cancer immunotherapy. J Exp Clin Cancer Res. 2021;40(1):267. doi: 10.1186/s13046-021-02068-5. PubMed PMID: 34433460; PubMed Central PMCID: PMCPMC8390200.
60. Zhu Y, Paniccia A, Schulick AC, Chen W, Koenig MR, Byers JT, et al. Identification of CD112R as a novel checkpoint for human T cells. J Exp Med. 2016;213(2):167-76. doi: 10.1084/jem.20150785. PubMed PMID: 26755705; PubMed Central PMCID: PMCPMC4749091.
61. Joshi CJ, Ke W, Drangowska-Way A, O'Rourke EJ, Lewis NE. What are housekeeping genes? PLoS Comput Biol. 2022;18(7):e1010295. doi: 10.1371/journal.pcbi.1010295. PubMed PMID: 35830477; PubMed Central PMCID: PMCPMC9312424.
62. Chen YC, Chang SC, Lee YS, Ho WM, Huang YH, Wu YY, et al. TOMM40 Genetic Variants Cause Neuroinflammation in Alzheimer's Disease. Int J Mol Sci. 2023;24(4). doi: 10.3390/ijms24044085. PubMed PMID: 36835494; PubMed Central PMCID: PMCPMC9962462.
63. Linnertz C, Anderson L, Gottschalk W, Crenshaw D, Lutz MW, Allen J, et al. The cis-regulatory effect of an Alzheimer's disease-associated poly-T locus on expression of TOMM40 and apolipoprotein E genes. Alzheimers Dement. 2014;10(5):541-51. doi: 10.1016/j.jalz.2013.08.280. PubMed PMID: 24439168; PubMed Central PMCID: PMCPMC4098029.
64. Filograna R, Mennuni M, Alsina D, Larsson NG. Mitochondrial DNA copy number in human disease: the more the better? FEBS Lett. 2021;595(8):976-1002. doi: 10.1002/1873-3468.14021. PubMed PMID: 33314045; PubMed Central PMCID: PMCPMC8247411.
65. Liou CW, Chen SH, Lin TK, Tsai MH, Chang CC. Oxidative Stress Biomarkers and Mitochondrial DNA Copy Number Associated with APOE4 Allele and Cholinesterase Inhibitor Therapy in Patients with Alzheimer's Disease. Antioxidants (Basel). 2021;10(12). doi: 10.3390/antiox10121971. PubMed PMID: 34943074; PubMed Central PMCID: PMCPMC8750673.
66. Mathew A, Lindsley TA, Sheridan A, Bhoiwala DL, Hushmendy SF, Yager EJ, et al. Degraded mitochondrial DNA is a newly identified subtype of the damage associated molecular pattern (DAMP) family and possible trigger of neurodegeneration. J Alzheimers Dis. 2012;30(3):617-27. doi: 10.3233/JAD-2012-120145. PubMed PMID: 22460333.
67. Wilkins HM, Weidling IW, Ji Y, Swerdlow RH. Mitochondria-Derived Damage-Associated Molecular Patterns in Neurodegeneration. Front Immunol. 2017;8:508. doi: 10.3389/fimmu.2017.00508. PubMed PMID: 28491064; PubMed Central PMCID: PMCPMC5405073.
68. Dekker J, Rippe K, Dekker M, Kleckner N. Capturing chromosome conformation. Science. 2002;295(5558):1306-11. doi: 10.1126/science.1067799. PubMed PMID: 11847345.
69. Lieberman-Aiden E, van Berkum NL, Williams L, Imakaev M, Ragoczy T, Telling A, et al. Comprehensive mapping of long-range interactions reveals folding principles of the human genome. Science.

2009;326(5950):289-93. doi: 10.1126/science.1181369. PubMed PMID: 19815776; PubMed Central PMCID: PMCPMC2858594.

70. Dixon JR, Selvaraj S, Yue F, Kim A, Li Y, Shen Y, et al. Topological domains in mammalian genomes identified by analysis of chromatin interactions. Nature. 2012;485(7398):376-80. doi: 10.1038/nature11082. PubMed PMID: 22495300; PubMed Central PMCID: PMCPMC3356448.
71. Nora EP, Lajoie BR, Schulz EG, Giorgetti L, Okamoto I, Servant N, et al. Spatial partitioning of the regulatory landscape of the X-inactivation centre. Nature. 2012;485(7398):381-5. doi: 10.1038/nature11049. PubMed PMID: 22495304; PubMed Central PMCID: PMCPMC3555144.
72. Sexton T, Yaffe E, Kenigsberg E, Bantignies F, Leblanc B, Hoichman M, et al. Three-dimensional folding and functional organization principles of the Drosophila genome. Cell. 2012;148(3):458-72. doi: 10.1016/j.cell.2012.01.010. PubMed PMID: 22265598.
73. Zhan Y, Mariani L, Barozzi I, Schulz EG, Bluthgen N, Stadler M, et al. Reciprocal insulation analysis of Hi-C data shows that TADs represent a functionally but not structurally privileged scale in the hierarchical folding of chromosomes. Genome Res. 2017;27(3):479-90. doi: 10.1101/gr.212803.116. PubMed PMID: 28057745; PubMed Central PMCID: PMCPMC5340975.
74. Sun F, Chronis C, Kronenberg M, Chen XF, Su T, Lay FD, et al. Promoter-Enhancer Communication Occurs Primarily within Insulated Neighborhoods. Mol Cell. 2019;73(2):250-63 e5. doi: 10.1016/j.molcel.2018.10.039. PubMed PMID: 30527662; PubMed Central PMCID: PMCPMC6338517.
75. Bendl J, Hauberg ME, Girdhar K, Im E, Vicari JM, Rahman S, et al. The three-dimensional landscape of cortical chromatin accessibility in Alzheimer's disease. Nat Neurosci. 2022;25(10):1366-78. doi: 10.1038/s41593-022-01166-7. PubMed PMID: 36171428; PubMed Central PMCID: PMCPMC9581463.
76. Li K, Chi R, Liu L, Feng M, Su K, Li X, et al. 3D genome-selected microRNAs to improve Alzheimer's disease prediction. Front Neurol. 2023;14:1059492. doi: 10.3389/fneur.2023.1059492. PubMed PMID: 36860572; PubMed Central PMCID: PMCPMC9968804.